With these thoughts in mind, the shift factors were also plotted according to the W-L-F relationship (Eq. 6) in Fig. 6. The ideal W-L-F curve generated with the "universal" constants of $C_1 = 17.4$ and $C_2 = 51.6$ is also presented in Fig. 6 for comparison. The "universal" constants do not hold for many polymers, and it is apparent that the experimentally obtained plot of $\log a_T$ *versus* $(T - T_R)$ for anhydrous lanolin does not lie where the W-L-F relationship (with "universal" constants) predicts. The lack of fit of the experimental data with the W-L-F prediction also suggests that the transition is probably not a glass transition as most polymers that undergo a glass transition obey the W-L-F prediction.

CONCLUSION

It has been demonstrated that the energy of activation for the structural changes occurring in the transition of anhydrous lanolin between 10 and 15° can be calculated by a temperature–shear frequency reduction scheme and an Arrhenius-type relationship. The E_a, which is ~90 kcal, compares favorably with the magnitude of the E_a of a high molecular weight polymer undergoing a glass transition. This comparison is significant when one considers the generally low molecular weight composition of anhydrous lanolin. The magnitude of the E_a for anhydrous lanolin suggests that the intra- and intermolecular forces are as great as those in high molecular weight polymers. Hence, the nature of the functional groups and the chain length of the molecules determine the strength of the structure of the system.

Overall, the experimental data suggest that anhydrous lanolin undergoes a major mechanical transition between 10 and 15°. Both the ability to superpose modulus *versus* shear frequency data and an E_a of 90 kcal for the transition are characteristic of a glass transition, but other observations are not. As described in the preceding paper (5), these observations are: a lower limiting value of the elastic modulus than would be expected for a glass transition, a slower rate of change of tan δ with temperature about the transition than would be expected for a glass transition, and a lack of fit of experimental data to the W-L-F relationship. Rather than a sharp transition from a rubbery to an ordered glassy state, it appears that anhydrous lanolin undergoes a mechanical transition from a rubber-like state to a structural state which is less ordered than a glassy state.

REFERENCES

(1) J. D. Ferry, "Viscoelastic Properties of Polymers," 3nd ed., Wiley, New York, N.Y., 1980.

(2) L. E. Nielsen, "Mechanical Properties of Polymers," vol. 1, Dekker, New York, N.Y., 1974.

(3) A. N. Martin, G. S. Banker, and A. H. C. Chun, "Advances in Pharmaceutical Sciences," vol. 1, H. S. Bean, A. H. Beckett, and J. E. Carless, Eds., Academic, New York, N.Y., 1964, p. 1.

(4) B. W. Barry, "Advances in Pharmaceutical Sciences," vol. 4, H. S. Bean, A. H. Beckett, and J. E. Carless, Eds., Academic, New York, N.Y., 1974, p. 1.

(5) G. W. Radebaugh and A. P. Simonelli, *J. Pharm. Sci.*, **72**, 415 (1983).

(6) J. J. Aklonis, W. J. MacKnight, and M. Shen, "Introduction to Polymer Viscoelasticity," Interscience, New York, N.Y., 1972.

(7) J. Bischoff, E. Catsiff, and A. V. Tobolsky, *J. Am. Chem. Soc.*, **74**, 3378 (1952).

(8) A. V. Tobolsky and J. R. McLoughlin, *J. Polymer Sci.*, **8**, 543 (1952).

(9) J. D. Ferry, *J. Colloid Sci.*, **10**, 474 (1955).

(10) J. R. Van Wazer, J. W. Lyons, K. Y. Kim, and R. E. Colwell, "Viscosity and Flow Measurements—A Laboratory Handbook of Rheology," Interscience, New York, N.Y., 1963.

(11) J. D. Ferry, *J. Am. Chem. Soc.*, **72**, 3746 (1950).

(12) R. C. Harper, H. Markovitz, and T. W. DeWitt, *J. Polymer Sci.*, **8**, 435 (1952).

(13) E. Catsiff and A. V. Tobolsky, *J. Colloid Sci.*, **10**, 375 (1955).

(14) M. L. Williams, R. F. Landel, and J. D. Ferry, *J. Am. Chem. Soc.*, **77**, 3701 (1955).

(15) N. L. Henderson, P. M. Meer, and H. B. Kostenbauder, *J. Pharm. Sci.*, **50**, 788 (1961).

ACKNOWLEDGMENTS

Adapted in part from a dissertation submitted by Galen W. Radebaugh to the University of Connecticut in partial fulfillment of the Doctor of Philosophy degree requirements.

Partially supported with funds from the Connecticut Research Foundation.

Reverse Permeation of Salicylate Ion Through Cellulose Membrane

FUJIO KAMETANI ˣ, SHUJI KITAGAWA, and HULKI A. GENCAY

Received December 21, 1981 from the *Faculty of Pharmaceutical Sciences, University of Tokushima, Shomachi, Tokushima 770, Japan.* Accepted for publication August 9, 1982.

Abstract □ The reverse permeation of salicylate ion and the effect of bovine serum albumin on the permeation were studied in a sodium salicylate–sodium oxalate–water system. In passive transport the permeation flux of an ion is expressed by the linear combination of the two terms which represent the concentration and electric potential gradients. Because the mobility of the sodium ion is greater than the oxalate ion, salicylate ion moves against the concentration gradient, and follows the electric potential gradient in the initial stage of permeation. The reverse permeation of salicylate ion through a cellulose membrane was accelerated with a high concentration ratio of oxalate to salicylate ions and reached a maximum value after 10 hr in the absence of bovine serum albumin. After reaching a maximum value, the salicylate ion permeated along the concentration gradient. The maximum concentration efficiency was 11.2%. In the presence of bovine serum albumin, the reverse permeation of salicylate ion reached a maximum value after 3 hr.

Keyphrases □ Reverse permeation—of salicylate ion with oxalate ion, through a cellulose membrane, protein effect on permeation flux □ Salicylate ion—permeation through a cellulose membrane, concentration by oxalate ion, protein effect on permeation flux □ Oxalate ion—permeation through a cellulose membrane with salicylate ion, protein effect on permeation flux

Most organic drugs dissociate in aqueous solutions and exist in ionic forms under biological conditions. Salicylate ion, one of the most commonly used drugs for analgesia, displaces other drugs such as the sulfonylureas (1) and sulfonamides (2), from the binding sites of the serum proteins. It has been reported that the absorption of salicylic acid is 61% in 0.1 *N* hydrochloric acid, 13% in sodium bicarbonate (pH 8) from the rat stomach (3), and 60% in physiological solution from the rat intestine (4). Effect of buffer constituents on salicylate absorption was studied with everted rat intestine and the inhibitory effect of potassium ions was reported (5–8). Since a variety of sub-

0022-3549/83/0400-0425$01.00/0

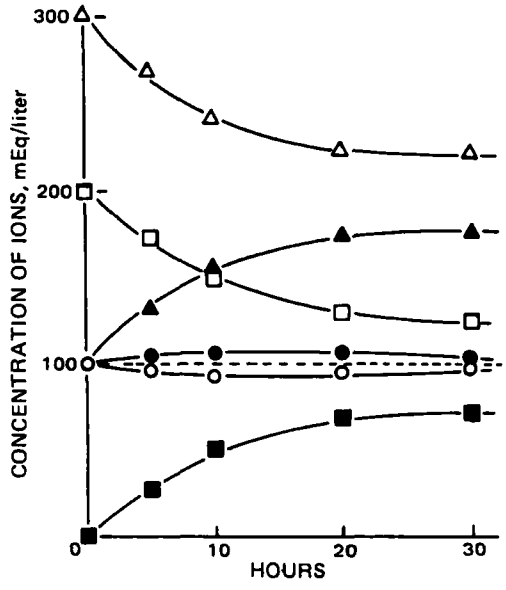

Figure 1—*Permeation of salicylate (○), oxalate (□), and sodium (△) ions. Initial concentration of sodium salicylate in compartments I and II was 100 mM; concentration of sodium oxalate in compartment I was 50 mM. Open figures represent compartment I; closed figures represent compartment II.*

stances are added to control the physical and physiological conditions of drug solutions, the absorption of drugs is affected by these multi-ionic components.

In passive transport at constant temperature, the membrane permeation flux of any ion (J_i) is given by the following equation which consists of two terms involving the concentration gradient and the electric potential gradient (9):

$$J_i = -D_i(\delta[i]/\delta x) - B_i Z_i[i](\mathrm{F/N})(\delta E/\delta x) \quad \text{(Eq. 1)}$$

where $[i]$ is the concentration of an ion i, E is the electric potential, and x is the coordinate taken in a direction of the permeation flux. D_i, B_i, F, N, and Z_i are the diffusion coefficient, the mobility, the faraday, Avogadro's number, and the valence of the ion, respectively. For the steady state of permeation, the following equation was derived from Eq. 1 (9):

$$J_i = -D_i(\delta[i]/\delta x) + \frac{B_i Z_i[i]}{\Sigma Z_j^2 B_j[j]} \Sigma Z_j D_j(\delta[j]/\delta x) \quad \text{(Eq. 2)}$$

where $[j]$ is the concentration of the coexisting ion j. Thus,

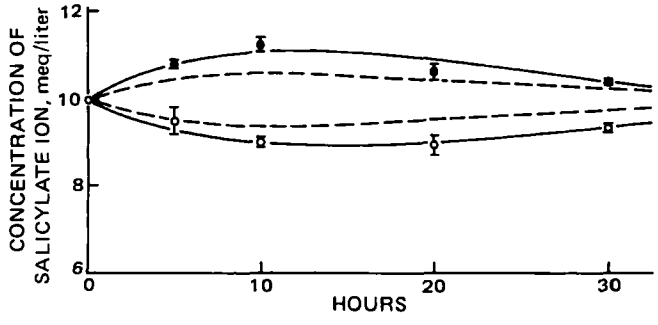

Figure 2—*Reverse permeation of salicylate ion. Initial concentration of sodium salicylate in compartments I and II was 10 mM; concentration of sodium oxalate in compartment I was 50 mM. Data points show the mean concentrations; standard deviations of four runs are indicated as bars on the data points. Key: (○) compartment I, (●) compartment II, and (- - -) values predicted from Eq. 5.*

Table I—Electric Potential Differences (ΔE)

Hours of Permeation	ΔE, mV
0	23.6
5	11.1
10	5.8
20	1.6
30	0.7

the apparent diffusion coefficient (D_i') is expressed as follows (10):

$$D_i' = kTB_i\left\{1 - \frac{Z_i[i]\Sigma Z_j B_j(\delta[j]/\delta x)}{(\Sigma Z_j^2 B_j[j])(\delta[i]/\delta x)}\right\} \quad \text{(Eq. 3)}$$

where k is the Boltzmann constant, T is the absolute temperature, and Σ means a sum of all ions. If the second term in the bracket is >1, D_i' is negative and reverse diffusion is observed in simple inorganic systems (10, 11).

In this report, the reverse permeation of salicylate ion was studied in a sodium salicylate–sodium oxalate–water system. Since oxalic acid is injected intravenously as a hemostatic agent for animals, sodium oxalate was used as a coexisting anion in this model system. The reverse permeation of salicylate ion was also studied in the presence of bovine serum albumin. Due to the reverse permeation, salicylate ion was concentrated in one compartment of the permeation cell. The concentration efficiency of salicylate ion varied with the concentration of oxalate ion.

EXPERIMENTAL

Materials and Permeation Procedures—The cellulose membrane used was 35-μm thick seamless cellulose tubing[1] purchased from a commercial source. Sodium salicylate, sodium oxalate, and sucrose were analytical grade[2]. Bovine serum albumin was purchased from a commercial source[3]. Distilled and deionized water was used for all experiments.

Permeation of salicylate ion was measured in four cells, as previously described (12). Each cell compartment was stirred by a magnet at ~900

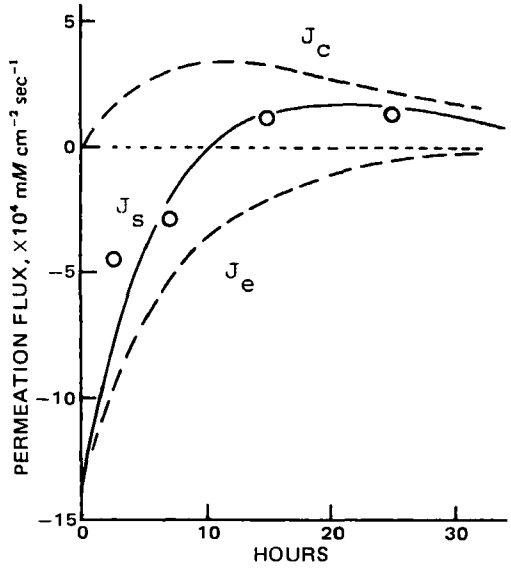

Figure 3—*Permeation flux of salicylate ion. Initial concentration of sodium salicylate and sodium oxalate are as shown in Fig. 2. Key: (J_s) total flux of salicylate ion, (J_c) flux of concentration gradient, (J_e) flux of electric potential gradient, and (○) as calculated by Eq. 4.*

[1] Union Carbide Corp., New York, N. Y.
[2] Wako Pure Chemical Industries, Osaka, Japan.
[3] Sigma Chemical Co., St. Louis, Mo.

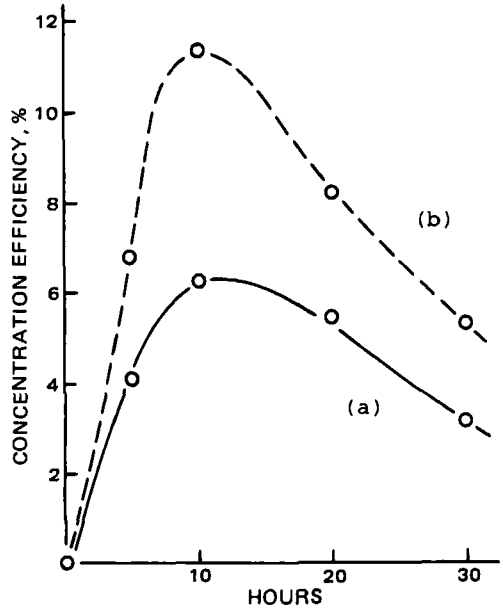

Figure 4—*Concentration efficiency of salicylate ion. Initial concentrations of sodium salicylate and sodium oxalate for (a) and (b) are as shown in Figs. 1 and 2, respectively.*

rpm at 25 ± 0.1°. In the presence of bovine serum albumin, the permeation of salicylate ion was followed in a cell where the volume of compartments I and II were 15.4 and 14.3 cm^3, respectively, and the membrane area was 3.19 cm^2. Sucrose was added to the solution without bovine serum albumin to make it isotonic. Both compartments were stirred at ~900 rpm at 10 ± 0.1°. The initial concentration of sodium salicylate was either 100 m*M* in both compartments with a 50 m*M* sodium oxalate solution in compartment I, or 10 m*M* in both compartments, with a 50 m*M* sodium oxalate solution in compartment I.

Analysis—Salicylate ion was analyzed by second differential absorption spectroscopy using a double-beam spectrophotometer[4] equipped with a derivative unit[5]. The second differential absorption spectrum ($\Delta\lambda$ = 4 nm) of the salicylate ion can be separated from that of oxalate ion. Sodium ion was analyzed with a flame photometer[6]. The concentration of oxalate ion was calculated from the difference of the concentrations of salicylate and sodium ions, on the assumption that the solution was electrically neutral. The diffusion potential through a membrane was measured with a DC-microvoltmeter[7] and calomel electrodes[8] using 3.3 *M* KCl agar bridges which contacted both cell compartments.

RESULTS AND DISCUSSION

The permeation of salicylate through a cellulose membrane in a mixed solution of sodium salicylate and sodium oxalate was measured at various times. The change in the concentration of ions where the initial concentration ratio of oxalate to salicylate in compartment I was 0.5, is shown in Fig. 1. The difference in concentration of salicylate ions in both compartments was zero at the initial stage of permeation and reached a maximum value after 10 hr. At this stage, salicylate ion was moving against the concentration gradient, *i.e.*, the salicylate ion concentration was increasing in compartment II. After the maximum reverse permeation, the concentration of salicylate ion reached the equilibrium concentration, equal to the initial concentration.

Assuming that the concentration gradient in the membrane is linear, the permeation flux can be calculated by the following equation (instead of Eq. 2):

$$J_i = -fkTB_ih_i\left\{\left(\frac{[i]_{II}-[i]_I}{L}\right)-\frac{Z_i[i]\Sigma Z_jB_jh_j([j]_{II}-[j]_I)/L}{h_i\Sigma Z_j^2B_j[j]}\right\} \quad \text{(Eq. 4)}$$

where f is the membrane constant, L is the thickness of the membrane,

[4] Model UV-180, Shimadzu Seisakusho, Kyoto, Japan.
[5] Model DES-2, Shimadzu Seisakusho, Kyoto, Japan.
[6] Type 205, Hitachi, Tokyo, Japan.
[7] Model PM-18C, Toa Electronics, Tokyo, Japan.
[8] Type 2010A, Hitachi-Horiba, Tokyo, Japan.

Table II—Initial Concentrations of Simple Permeation

Type[a]	Compartment	Sodium Salicylate, m*M*	Sodium Oxalate, m*M*
a	I	0.2	90
	II	0.4	10
b	I	0.2	10
	II	0.4	90
c	I	0.2	50
	II	0.4	50

[a] Taken from the text.

and h_i is a coefficient for the activity coefficient (γ_i) of the ion such that $h_i = 1 + \delta\ln\gamma_i/\delta\ln[i]$. Using the Güntelberg equation (13) for γ_i, the concentration of salicylate ion in compartment II was calculated by:

$$[s]_{II}^{t+\Delta t} = [s]_{II}^{t} + J_sAt/V_{II} \quad \text{(Eq. 5)}$$

In this calculation, $[s]_{II}^{t}$ and $[s]_{II}^{t+\Delta t}$ are the concentrations of salicylate ion in compartment II after t and $t + \Delta t$ hours, respectively, J_s is the permeation flux of salicylate ion, A is the membrane area, and V_{II} is the volume of compartment II. The constant (f), obtained with calcium chloride, was 0.0573. B_i values for salicylate, oxalate, and sodium ions were 2.33×10^8, 2.35×10^8, and 3.24×10^8 (cm sec^{-1} $dyne^{-1}$), respectively, which were calculated from limiting equivalent conductivities (14) according to Wendt (15). Observed and calculated values are shown in Fig. 2 when the initial concentration ratio of oxalate to salicylate ions was 5. Since the sampling time interval in the initial stage was long compared with the permeation rate, the first permeation flux of salicylate ion was sooner than estimated. Therefore, calculated concentrations are smaller values than expected because of the cumulative addition in Eq. 5.

To clarify the difference between observed and calculated values, the electric potential differences (ΔE) were measured (Table I). Assuming that the potential gradient in the membrane is linear ($\delta E/\delta x = \Delta E/L$), permeation flux due to the electric potential gradient (J_e) can be calculated using the following equation instead of the second term in Eq. 4:

$$J_e = -fB_iZ_ih_i[i](F/N)(\delta E/\delta x) \quad \text{(Eq. 6)}$$

Adding J_e to the permeation flux due to the concentration gradient (J_c) calculated by the first term in Eq. 4, the total flux of salicylate ion is obtained, as shown in Fig. 3. In this case, the calculated values are in good agreement with the observed values. The negative total flux indicates reverse permeation, which is at a maximum when the total flux is equal to zero.

To compare the reverse permeation of salicylate ion under different conditions, a mean concentration ($\overline{[s]}$) and a mean value of concentration change ($\overline{\Delta[s]}$) of the salicylate ion were calculated by:

$$\overline{[s]} = \frac{V_I([s]_I^0 + [s]_I^f) + V_{II}([s]_{II}^0 + [s]_{II}^f)}{2(V_I + V_{II})} \quad \text{(Eq. 7)}$$

and

$$\overline{\Delta[s]} = \frac{V_I([s]_I^f - [s]_I^0) + V_{II}([s]_{II}^0 - [s]_{II}^f)}{V_I + V_{II}} \quad \text{(Eq. 8)}$$

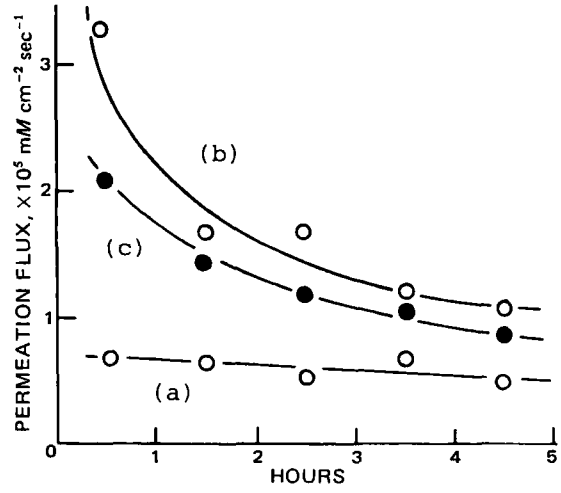

Figure 5—*Concentration gradient effect. Initial concentrations of sodium salicylate and sodium oxalate for (a), (b), and (c) are shown in Table II.*

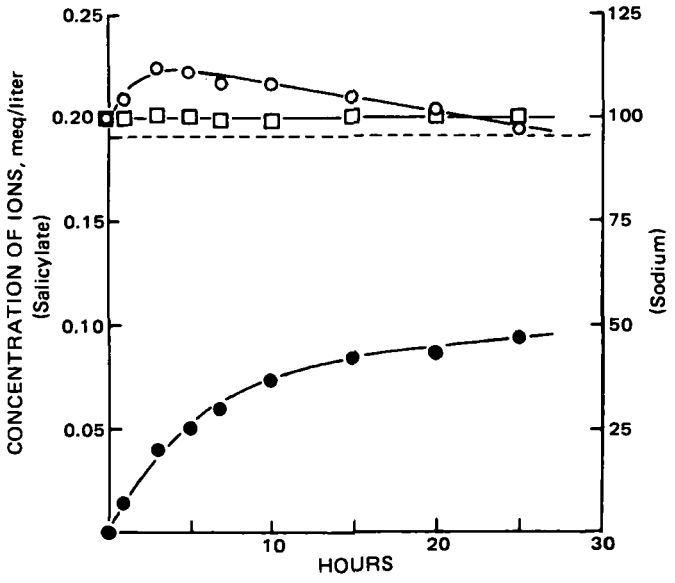

Figure 6—*Reverse permeation of salicylate ion in the presence of bovine serum albumin. Initial concentrations of sodium salicylate in compartment I and II were 0.2 and 0.4 m*M*, respectively; bovine serum albumin (0.1 m*M*) was dissolved in compartment II. Key: concentration of salicylate ion in compartment I when initial concentration of sodium oxalate in both compartments was 50 m*M *(□); concentration of salicylate (○) and sodium (●) ions in compartment I when initial concentrations of sodium oxalate in comparments I and II were 0 and 50 m*M*, respectively.*

where $[s]_I^0$ and $[s]_{II}^0$ are the initial concentrations of salicylate ion and $[s]_I^t$ and $[s]_{II}^t$ are the concentrations after time t in the indicated compartments. V_I and V_{II} are volumes of compartment I and II, respectively. In this study, the compartment of the permeation cell with a higher total concentration of salicylate ion is designated as II.

The efficiency of concentration (R) was calculated by:

$$R = -\overline{\Delta[s]}/\overline{[s]} \qquad \text{(Eq. 9)}$$

Since the numerator in Eq. 9 is negative due to the reverse permeation, a minus sign is added to the right-hand side of Eq. 9 to obtain a positive value for the efficiency of concentration. R-values at 10 hr were 6.1 and 11.2% when the initial concentration ratios of oxalate to salicylate were 0.5 and 5, respectively (Fig. 4).

To confirm the concentration gradient effect of the oxalate ion, the permeation fluxes of salicylate ion were measured under three different conditions: (*a*) the opposite direction from the concentration gradients of salicylate and oxalate ions, (*b*) the same direction as the concentration gradients, and (*c*) no concentration gradient of oxalate ion (Table II). The concentration ratio of oxalate to salicylate was greater than that used previously (Fig. 2) in order to obtain significant values for the permeation fluxes. The simple permeation of salicylate ion was accelerated most with both concentration gradients in the same direction (Fig. 5).

In the presence of bovine serum albumin, when the concentration of oxalate in both compartments was the same (*i.e.*, no concentration gradient of oxalate), a significant concentration change of salicylate was not obtained under the experimental conditions (Fig. 6). The slow permeation of the salicylate ion was due to the small membrane area and small concentration gradient. The concentration of unbound salicylate ion in compartment II would be lower than that in compartment I because of protein binding, which can be estimated by the binding parameters (16). Salicylate ion permeated from compartment II to I against the concentration gradient, with a greater concentration gradient of oxalate ion. Since it has been shown that association constants $>1 \times 10^4 M^{-1}$ affect drug distribution (17), salicylate ion bound on the secondary binding sites of bovine serum albumin can permeate with the electric potential gradient based on the oxalate concentration gradient. The reverse permeation reached a maximum value after 3 hr in the presence of bovine serum albumin. The concentration of salicylate ion in compartment I decreased after the maximum and approached the lower concentration (0.191 m*M*) which was obtained after 72 hr, as shown by the dotted line in Fig. 6. The concentration of sodium ion in compartment I showed that the solution had not equilibrated after 30 hr.

Organic drugs permeate through biomembranes mainly in their uncharged forms. If the same mechanism is applicable to biological systems, salicylate ion may be concentrated on the membrane boundary with the concentration gradient of coexisting ions. Assuming that the effective pH at the site of drug absorption is 5.3 (18), uncharged salicylic acid would be concentrated more on the membrane boundary than in the intestinal contents. When salicylate is coadministered with a weakly acidic drug, then the permeation rate of salicylate determined by dialysis techniques will vary with the concentration gradient of the coexisting drug.

REFERENCES

(1) K. F. Brown and M. J. Crooks, *Biochim. Pharmacol.*, **25,** 1175 (1976).

(2) H. Ichibagase, Y. Imamura, and H. Nakagami, *Chem. Pharm. Bull.*, **24,** 204 (1976).

(3) L. S. Schanker, P. A. Shore, B. B. Brodie, and C. A. M. Hogben, *J. Pharmacol. Exp. Ther.*, **120,** 528 (1957).

(4) L. S. Schanker, D. J. Tocco, B. B. Brodie, and C. A. M. Hogden, *ibid.*, **123,** 81 (1958).

(5) M. Mayersohn and M. Gibaldi, *J. Pharm. Sci.*, **58,** 1429 (1969).

(6) M. Mayersohn and M. Gibaldi, *Biochim. Biophys. Acta*, **196,** 296 (1970).

(7) L. Z. Benet, J. M. Orr, R. H. Turner, and H. S. Webb, *J. Pharm. Sci.*, **60,** 234 (1971).

(8) S. Kojima, T. Tenmizu, T. Shino, and M. Cho, *Chem. Pharm. Bull.*, **22,** 952 (1976).

(9) M. Nakagaki and M. Kobayashi, *Yakugaku Zasshi*, **93,** 287 (1973).

(10) M. Nakagaki and S. Kitagawa, *Bull. Chem. Soc. Jpn*, **49,** 1748 (1976).

(11) M. Nakagaki and S. Kitagawa, *Yakugaku Zasshi*, **98,** 840 (1978).

(12) F. Kametani, S. Kitagawa and K. Nishiyama, *Chem. Pharm. Bull.*, **27,** 2710 (1979).

(13) E. Güntelberg, *Z. Phys. Chem.*, **123,** 199 (1926).

(14) H. Landolt and R. Börnstein, "Zahlenwerte und Funktionen aus Astronomie, Geophysik und Technik," vol. 2, part 7, Springer-Verlag, Berlin, 1960, p. 257.

(15) R. P. Wendt, *J. Phys. Chem.*, **69,** 1227 (1965).

(16) C. A. Cruze and M. C. Meyer, *J. Pharm. Sci.*, **65,** 33 (1976).

(17) B. K. Martine, *Nature (London)*, **207,** 274 (1965).

(18) L. S. Schanker, "Fundamentals of Drug Metabolism and Drug Disposition," B. N. La Du, H. G. Mandel, and E. L. Way, Eds., Williams & Wilkins, Baltimore, Md., 1972, p. 29.